Recognition of a Pre-tRNA Substrate by the *Bacillus subtilis* RNase P Holoenzyme†

Andrew Loria,‡ S. Niranjanakumari,§ Carol A. Fierke,§ and Tao Pan*,‡

Department of Biochemistry & Molecular Biology, University of Chicago, Chicago, Illinois 60637, and Department of Biochemistry, Duke University Medical Center, Durham, North Carolina 27710

Received July 10, 1998; Revised Manuscript Received August 28, 1998

ABSTRACT: The holoenzyme of the bacterial RNase P has broader selectivity for biological substrates compared to the RNA alone (denoted P RNA) reaction. The structural basis of the substrate selectivity is investigated using a pre-tRNA substrate containing single-atom modifications by single turnover kinetics. Hydroxyl radical protection of the holoenzyme in the absence of the substrate shows that the RNase P protein binds to several regions in P RNA. The holoenzyme interacts with a subset of functional groups in the T stem-loop region of a pre-tRNA substrate previously identified to directly contact P RNA. The subtle change in structural recognition allows the holoenzyme to recognize RNA structures with only a small perturbation in an A-form helix at the corresponding position of the T stem-loop. This altered profile may permit the holoenzyme to bind non-tRNA substrates with little change in catalytic efficiency. The holoenzyme recognizes the same set of functional groups as the P RNA reaction in the region around the cleavage site and shows similar cleavage site selection compared to the P RNA reaction. These results suggest that the holoenzyme does not alter the fundamental mechanism of this enzymatic reaction. Rather, the holoenzyme significantly affects the binding affinity of an RNA substrate through additional interactions with the 5′ leader [Kurz, C. A., Niranjanakumari, S., and Fierke, C. A. (1998) *Biochemistry 37,* 2393] and through altered recognition of the substrate structure.

RNase P is an essential enzyme involved in producing the mature 5′ end of all tRNAs through a site-specific endonucleolytic cleavage reaction (*1, 2*). The holoenzyme of the bacterial RNase P is composed of one large RNA of ∼330−420 nucleotides (denoted P RNA) and one small protein (13−15 kDa) subunit. Under physiological conditions (i.e., <10 mM Mg^{2+} and <0.2M monovalent ions), the k_{cat}/K_m of the RNA alone reaction is 3−4 orders of magnitude lower than the reaction catalyzed by the holoenzyme (ref 3; A.L. and T.P., unpublished material). This difference in catalytic efficiency has been recently attributed to the significantly enhanced holoenzyme interactions with the 5′ leader (*3, 4*). The rate constant for the release of the tRNA product remains comparable under physiological conditions for both P RNA and holoenzyme reactions (*3*).

The structural role of the RNase P protein has also been an active area of investigation. Hydroxyl-radical protection of bacterial P RNAs has shown that the ribozyme component is folded under physiological conditions in the absence of the P protein (*5, 6*). Although the folded P RNA efficiently catalyzes the cleavage of an in vitro selected substrate that binds at an alternate site (*7*), P RNA at low ionic strength does not optimally bind and cleave pre-tRNA substrates. On the basis of the protection of the RNA component from chemical modifications and hydroxyl radical attack upon protein binding, Westhof and Altman proposed that binding of the RNase P protein stabilizes a catalytically more efficient conformation of the P RNA (*8*−*10*). There is, however, little additional physical evidence for this proposed holoenzyme conformation. An alternative explanation suggested in the literature (*11*) is that the protein component alleviates charge repulsion, perhaps by enhancing the affinity of cation-binding sites.

Compared to the P RNA reaction, the holoenzyme also catalyzes the cleavage of a broader array of substrates. For example, the holoenzyme is much more efficient in processing the precursor of the 4.5S RNA from *Escherichia coli* (*12*). In contrast to pre-tRNA substrates, high ionic conditions do not restore high efficiency of pre-4.5S RNA processing catalyzed by P RNA. Furthermore, a larger variety of efficient substrates were isolated by in vitro selection using the *E. coli* holoenzyme than P RNA alone (*13*). These results suggest that the recognition of RNA substrates by the holoenzyme is altered.

This paper examines aspects of the structure and substrate recognition of the *Bacillus subtilis* holoenzyme. Hydroxyl radical footprinting shows that binding of the P protein only moderately decreases the concentration of Mg^{2+} at which half of the P RNA molecules are folded ($K_{1/2}^{[Mg]}$) with no change in the Hill coefficient. Using a substrate containing a 2′ deoxy at the cleavage site (*14*), effects of substrate modification on binding and the chemical step were determined. The major difference between the P RNA and the holoenzyme recognition resides in their interactions with the 5′ leader sequence (*3, 4*) and the T stem-loop region of a pre-tRNA substrate. This altered binding mode allows the holoenzyme to bind a broader range of RNA structures with similar affinity.

† This work was supported by grants from the NIH (GM52993 to T.P., GM55387 to C.A.F.) and the American Cancer Society (JFRA-543 to T.P.).

* Corresponding author. Tel: (773) 702-4179. Fax: (773) 702-0439. E-mail: taopan@midway.uchicago.edu.

10.1021/bi9816507 CCC: $15.00
Published on Web 10/14/1998

MATERIALS AND METHODS

Preparation of the RNase P Holoenzyme and the Pre-tRNA Substrates. The *B. subtilis* P protein was overexpressed and purified from *E. coli* as described (*15*). To reconstitute the holoenzyme, the *B. subtilis* P RNA transcript was heated in the reaction buffer without Mg^{2+} at 90 °C for 2 min, followed by incubation at ambient temperature for 3 min. $MgCl_2$ was then added to appropriate concentrations and the P RNA was further incubated at 50 °C for 10 min to ensure complete renaturation (*16*). Equal moles of P protein were then added to the renatured P RNA and the mixture further incubated at 37 °C for 5 min. All holoenzyme concentrations used in this work were at least 10 times higher than the K_d of the *B. subtilis* holoenzyme (~0.4 nM at 20 mM HEPES, pH 8.0, 400 mM NH_4OAc, 10 mM $MgCl_2$, 0.01% Nonidet P-40, and 5% glycerol, 37 °C; from ref *8*).

RNA substrates were prepared by either single or double ligation of synthetic oligoribonucleotides to an RNA transcript containing nucleotides 10−76 or 10−52 of yeast $tRNA^{Phe}$ as described previously (*14, 17*). Except for the oligonucleotide containing 5-methyl-iso-cytidine (isoC), the RNA oligonucleotides were custom synthesized by Dharmacon Research (Boulder, CO) using novel 2′ protecting groups (*18*). The isoC phosphoramidite was synthesized as described (*19*), and the oligonucleotide containing isoC was synthesized using standard phosphoramidite chemistry (*20*).

Fe(II)-EDTA Footprinting of the Holoenzyme. The basic protocol for the hydroxyl radical protection of *B. subtilis* P RNA was described in ref *5*. The holoenzyme was reconstituted as described above at a final concentration of 0.1 μM. Products of the Fe(II)-EDTA footprinting were separated on 15 and 6% polyacrylamide gels containing 7 M urea. A protection factor for each residue was defined as the amount of radioactivity in each product band without Mg^{2+} divided by the amount of radioactivity in each band with varying concentrations of Mg^{2+}. Only residues with protection factor of >1.5 at 10 mM $MgCl_2$ are designated as protected against hydroxyl radical attack. To assign P protein dependent protection, the protection factor at each position in P RNA in the presence of P protein was divided by the protection factor in the absence of P protein. Only residues with this ratio of >1.5 at 10 mM $MgCl_2$ are designated as protected upon P protein binding.

Kinetics of the Cleavage Reaction. All kinetic reactions were performed under single turnover conditions with 10−10000-fold molar excess of holoenzyme over 5′ ^{32}P-labeled substrates. The final concentrations of the holoenzyme range from 0.005 to 25 μM, always at 1 mol of P RNA/1 mol of P protein. Unless noted otherwise, all reactions were carried out in 50 mM MES or HEPES, pH 6.1−7.3, 10 mM $MgCl_2$, and 2% glycerol at 37 °C. The details of kinetic reactions and data processing are identical to those described in ref *16*. Cleavage sites at the correct and incorrect positions are designated as c^0, m^2 and m^{-1}-site, respectively. For every substrate, the maximum cleavage rate constant, $k^{c^0/m^2/m^{-1}}$, and the ribozyme concentration, K^{c^0}, at which the cleavage rate constant equals to $k^{c^0}/2$ are determined.

A pulse chase experiment with the C/G-rich substrate containing a 2′ deoxy at the c^0-site was carried out to ensure that the rate of substrate dissociation, k_{-1}, is greater than the rate of cleavage, k_2. Cleavage with ~0.1 μM holoenzyme ($\sim K^{c^0}$) and trace amount of ^{32}P-labeled substrate was allowed to proceed for 1.5 or 3.5 min at which time *E. coli* tRNA mixture (Type XX from Sigma Co.; ref *21*) was added to a final concentration of 68 μM. The addition of tRNA mixture resulted in a 1.5-fold dilution in the holoenzyme concentration. Only buffer and $MgCl_2$ were added in the control reaction. Cleavage was then allowed to proceed to 40 min ($\sim 11 t_{1/2}$ for the control reaction). The K_I of this tRNA mixture is 3 ± 1 μM (data not shown) under our conditions, so the cleavage reaction is expected to be inhibited by ~23-fold when $k_{-1} > k_2$.

RESULTS

Fe(II)-EDTA Footprinting of the Holoenzyme. Hydroxyl radical protection of the holoenzyme compared to that of P RNA reveals nucleotide residues that are involved in either direct contacts with the P protein or in a conformational change upon P protein binding (Figure 1A). Although substantial protection of *B. subtilis* P RNA is observed in the absence of the P protein, P protein binding enhances and induces protection of a large number of P RNA residues (Figure 1B). A large block of protected residues may indicate a direct contact area for P protein, although it is unlikely that all of the residues in these areas are protected by direct contacts. Using this criterion, three areas in P RNA can be tentatively assigned as contacting the P protein (circled numbers in Figure 1B). These contact areas are located in both folding domains of P RNA (*5, 6*); however, no P protein dependent protection is observed using either domain constructs (data not shown). Therefore, P protein must bind simultaneously to both domains in order to protect specific P RNA residues.

P protein binding only moderately decreases the Mg^{2+} concentration required to fold the tertiary structure of P RNA (Figure 2). In the absence of P protein and no added monovalent ions, P RNA folds with a $K_{1/2}^{[Mg]}$ of 3.1 ± 0.2 mM and a Hill coefficient of 3.2 ± 0.2 (*5*). P protein binding improves $K_{1/2}^{[Mg]}$ to 2.1 ± 0.3 mM with an identical Hill coefficient (3.4 ± 0.4). These results suggest that the P protein does not significantly affect the stability of the tertiary structure of P RNA as detected by hydroxyl radical protection. P protein binding to both domains may change the global juxtaposition of these domains. Such global conformational change may either be undetectable by hydroxyl radical protection or be observed as protected residues when P protein binds. These data confirm that the main function of the P protein is not for stabilization of the global fold of P RNA (*3*).

pH Dependence of the Holoenzyme Reaction. Two pre-$tRNA^{Phe}$ substrates with 5′ leaders of five nucleotides are used to characterize the holoenzyme reaction. The C/G-rich 5′ leader substrate has been used extensively in P RNA work (*14, 17*), whereas the A/U-rich 5′ leader substrate reflects the 5′ leader sequence composition of biological tRNA precursors. Unless otherwise noted, most substrates used in this work contain a 2′ deoxy nucleotide at the cleavage site which decreases the cleavage rate constant (k^{c^0}) by more than 20-fold for the holoenzyme reaction. The decreased cleavage rate constants allow estimation of substrate binding (K^{c^0} approximates K_d) and the chemical step (k^{c^0} proportional to k_2) in single turnover experiments. Similar to the P RNA

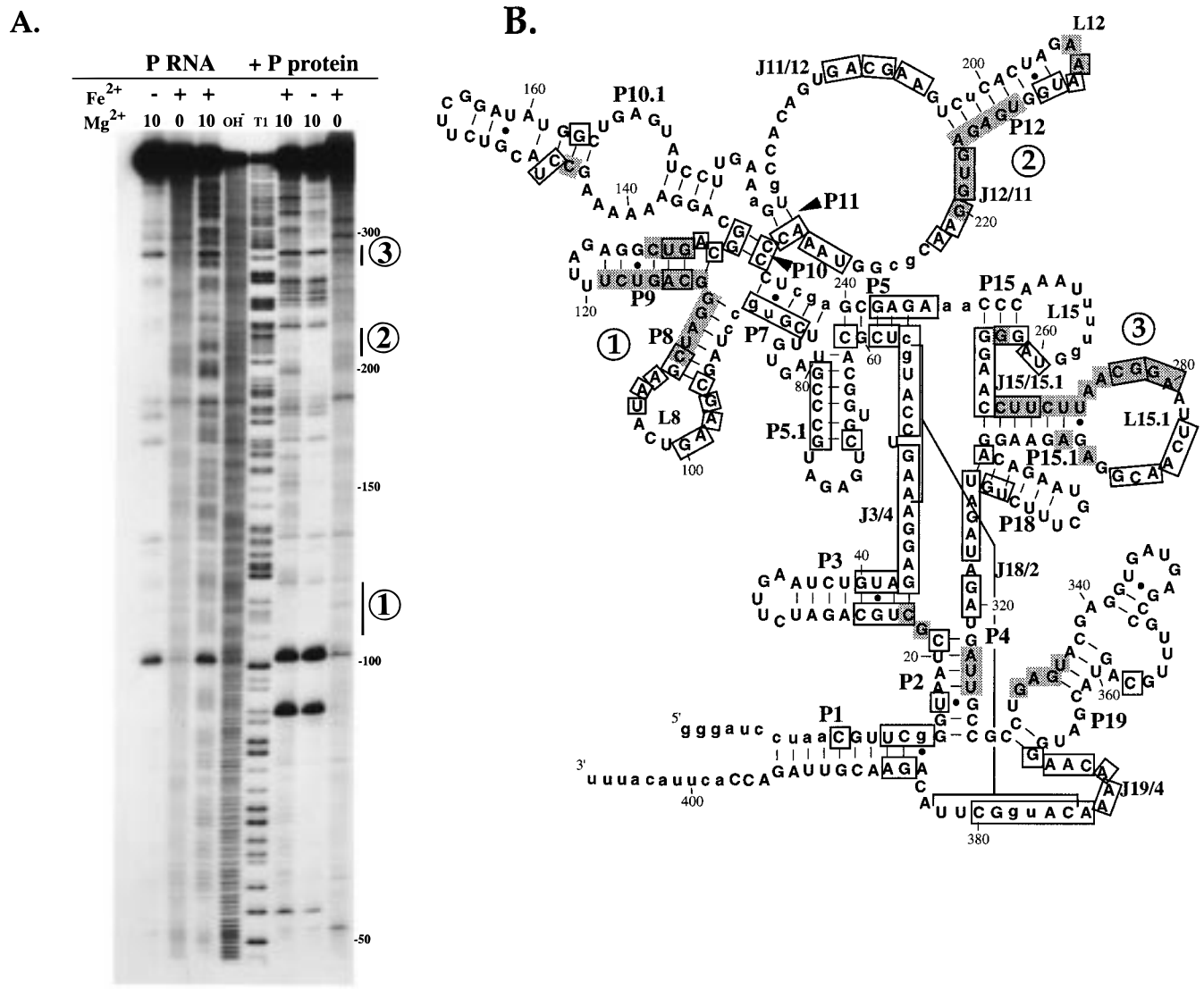

FIGURE 1: (A) Representative autoradiograph of Fe(II)-EDTA footprinting of the *B. subtilis* P RNA in the presence and absence of P protein. The particular experiment shown was carried out in 20 mM trisHCl, pH 7.5, 0 or 10 mM Mg^{2+}, 0.1 μM P RNA, and 0.1 μM P protein at 37 °C for 30 min. OH^- and T1: partial alkaline hydrolysis and nuclease T1 digestion of the same RNA. The P protein specific bands in the absence of Fe^{2+} (second lane from right) are present reproducibly; these bands may originate from Mg^{2+}-dependent hydrolysis of specific nucleotide positions that have altered conformations upon P protein binding. The potential contact areas 1−3 are marked by circled numbers (compare the third and the sixth lanes from right). (B) Summary of the Fe(II)-EDTA footprinting results using combined data obtained from six sequencing gels that enabled accurate analysis of different regions in P RNA. Nucleotides with a protection factor of >1.5 upon the addition of 10 mM $MgCl_2$ to P RNA in the absence of P protein are boxed (compare the second and the third lanes from left in panel A, quantitation from ref *5*). Nucleotides with relative protection factor of >1.5 upon the addition of P protein at 10 mM $MgCl_2$ are shaded (compare the third and the sixth lanes from left in panel A). The P protein potentially contacts three regions in the P RNA marked 1−3. Regions 1 and 2 are located in folding domain I (nucleotides 86−239), and region 3 is located in folding domain II (nucleotides 240−407 + 1−85). The nucleotides shown in lower cases cannot be analyzed due to gel resolution or the presence of Fe^{2+}-independent cleavage products.

reaction (*17*), k^{c^0} for both substrates is log-linearly dependent on pH (Figure 3A) and cleavage of the A/U-rich 5′ leader substrate is 4−5 times faster. A dependence of the cleavage rate constant on the 5′ leader sequence has also been observed for a pre-$tRNA^{Asp}$ substrate (*4*) where changing the 5′ leader from 5′GU to 5′GG decreases the cleavage rate constant by ∼60-fold. K^{c^0} for the C/G-rich 5′ leader substrate increases as the pH is lowered, proportional to the $[H^+]$ within the pH range tested (Figure 3B). In contrast, K^{c^0} for the A/U-rich substrate is much less dependent on pH. K^{c^0} for the C/G-rich 5′ leader substrate in the P RNA reaction is nearly independent of pH (*14*). Hence, the pH dependence of binding for the C/G-rich 5′ leader substrate is likely due to differential protonation of the 5′ leader region bound to the holoenzyme. Despite this pH dependence, we have used the C/G-rich 5′ leader substrate for subsequent work since its slower k^{c^0} and higher K^{c^0} allow a more accurate interpretation of k^{c^0} ($\approx k_2$) and K^{c^0} [$=(k_{-1} + k_2)/k_1 \approx K_d$ when $k_2 \ll k_{-1}$].

To test that the dissociation constant (k_{-1}) is greater than the chemical step (k_2) for the C/G-rich 5′ leader substrate, a pulse chase experiment was performed using the tRNA product as inhibitor (*21*). The holoenzyme (at a concentration similar to K^{c^0}) and substrate were allowed to react in the absence of chase for a time period to maximize the concentration of the enzyme−substrate complex. The tRNA product was then added and the reaction allowed to proceed to completion. The amount of tRNA product added is $\sim 22K_I$ for this reaction (data not shown) and the cleavage rate

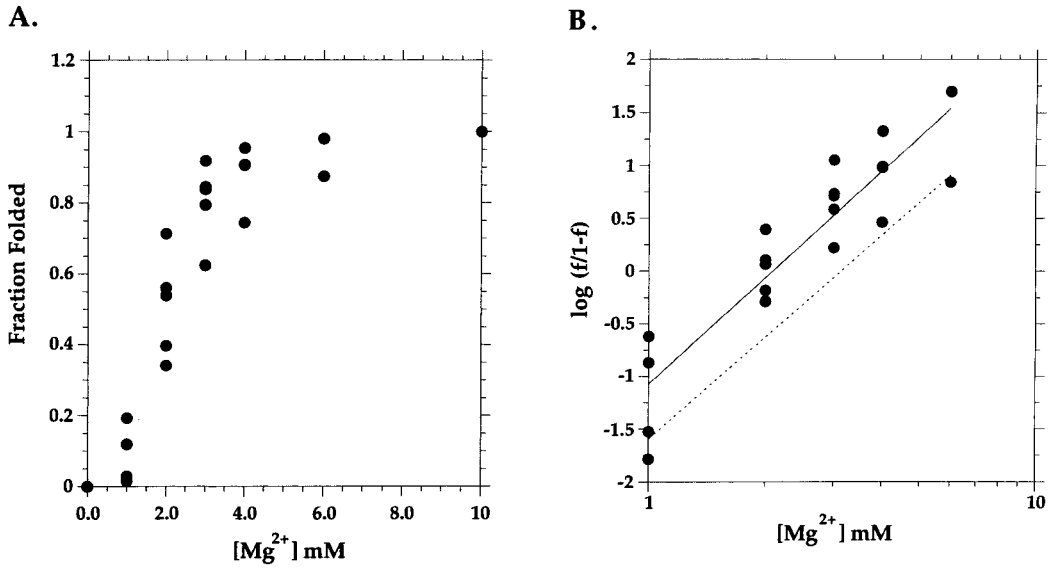

FIGURE 2: (A) Fraction of P RNA folded as a function of $[Mg^{2+}]$ in the presence of the P protein. The *y*-axis is normalized to zero in the absence of Mg^{2+} and to one at 10 mM $MgCl_2$. The composite protections of residues 45−47, 75−77, 96−98, 110−112 and 126−129 are shown. (B) Plot of $\log(f/1 - f)$ versus $[Mg^{2+}]$ from the data shown in panel A. The Mg^{2+} concentration at which 50% of P RNA are folded [designated as $K_{1/2}^{[Mg]}$(folding)] is 2.1 ± 0.3 mM. The Hill coefficient corresponds to the slope of the curve (3.4 ± 0.4). The dashed line represents the curve fitting for P RNA folding in the absence of the P protein (data from ref *5*).

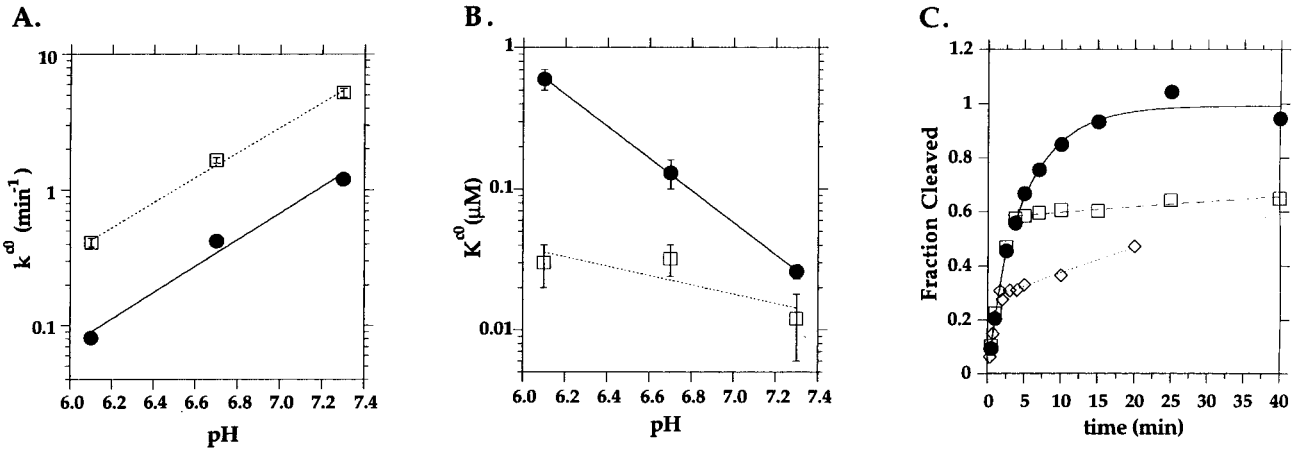

FIGURE 3: pH dependence of k^{c0} (A) and K^{c0} (B) of the holoenzyme reaction at 37 °C in 10 mM $MgCl_2$, 2% glycerol, 50 mM MES, pH 6.1, 6.7 or HEPES, pH 7.3. The substrate sequences are 5′ pCGCUdC-tRNA^{Phe} (●) and 5′ pAAUAdU-tRNA^{Phe} (□). For the cleavage rate, the pH dependence has a slope of 0.9−1.0 for both substrates. For K^{c0}, the pH dependence has a slope of −1.1 and −0.3 for the C/G-rich and A/U-rich substrates, respectively. The pH dependence of K^{c0} for the P RNA reaction at high ionic condition using the C/G-rich 5′ leader substrate has a slope of −0.2 (*14*). (C) Pulse-chase experiment using the C/G-rich 5′ leader substrate to determine $k_{-1} > k_2$. Cleavage was carried out at ∼0.1 μM holoenzyme before chase (●, $k_{obs} = 0.24 \pm 0.01$ min^{-1}) and <1 nM substrate for 1.5 (◇) or 3.5 (□) min in 50 mM MES, pH 6.7, 10 mM $MgCl_2$, and 2% glycerol at 37 °C. An *E. coli* tRNA mixture was then added to a final concentration of 68 μM (∼22K_I). Only buffer + $MgCl_2$ were added in the control reaction (●, $k_{obs} = 0.19 \pm 0.05$ min^{-1} after chase). The fit for the chase (dashed lines) correspond to ∼23-fold decreased reaction rate compared to the control.

constant after the addition of tRNA should be ∼23× slower when $k_{-1} > k_2$. This expected decrease in the cleavage rate constant is indeed observed (Figure 3C). If $k_2 > k_{-1}$, additional product reflective of the concentration of [ES] should form with a rate constant equal to k_2.

Substrate Modification in the T Stem-Loop Region of the tRNA. P RNA binding of the T stem-loop confers specificity for the pre-tRNA substrate. In the P RNA reaction, six functional groups in the T stem-loop region have been identified to directly interact with P RNA, each contributing 1.0−1.7 kcal/mol in binding (*14, 17*). Five of the six include the 2′OH of 53, 54, 61, 62, and the 4-NH_2 of C56, which are aligned within a groove-like structure dictated by the tertiary structure of tRNA (*14*). The 2′OH of 56 is on the other side of this groove and may represent a second surface in contacting P RNA. All six functional groups are modified and tested for an effect on the holoenzyme reaction (Table 1). The 2′OH → 2′H modification for nucleotides 53, 54, and 62 results in a loss of 1.5−1.9 kcal/mol in K^{c0}, suggesting that these 2′OH groups also contact the holoenzyme directly. On the other hand, the loss in binding for the 2′OH → 2′H modification of nucleotides 61 and 56 is much smaller, 0.3−0.6 kcal/mol. Furthermore, the a19u56 and c19g56 mutants fail to significantly affect binding or chemistry (Table 1). A more dramatic modification of C56 to isoC56 confirms that the interaction with C56 appears to be absent in the holoenzyme reaction. In addition, the c19g56 mutant incorporated into the A/U-rich 5′ leader substrate also has very little effect on binding and cleavage (Table 1). These results show that the holoenzyme only contacts a part of the

Table 1: Effects of Substrate Modifications in the T Stem-Loop Region and P RNA Mutations

substrate[a]	K^{c^0} (μM)[b]	$\Delta\Delta G$ (kcal/mol)[c]	k^{c^0} (min^{-1})[b]	$\Delta\Delta G$ (kcal/mol)[c]
(d-1)	0.13 ± 0.03		0.42 ± 0.04	
d53	2.7 ± 0.4	1.9	0.22 ± 0.01	0.4
d54	1.4 ± 0.6	1.5	0.29 ± 0.04	0.2
d62	2.6 ± 0.7	1.8	0.21 ± 0.02	0.4
d61	0.21 ± 0.10	0.3	0.17 ± 0.01	0.6
d56	0.37 ± 0.10	0.6	0.16 ± 0.02	0.6
a19u56	0.12 ± 0.02	0.0	0.27 ± 0.01	0.3
c19g56	0.31 ± 0.05	0.5	0.30 ± 0.02	0.2
a19isoC56	0.13 ± 0.03	0.0	0.27 ± 0.02	0.3
aaua(d)u[d]	0.032 ± 0.008	−0.9 (−)	1.6 ± 0.1	−0.8 (−)
aaua(d)u/c19g56[d]	0.040 ± 0.016	(0.1)	1.1 ± 0.1	(0.2)
g230	17 ± 6	3.0	0.016 ± 0.003	2.0
g130	4.1 ± 0.5	2.1	0.10 ± 0.01	0.9

[a] All substrates contain a 2′deoxy nucleotide (d-1) at the c^0-site and a C/G-rich 5′ leader sequence unless indicated otherwise. [b] Reaction conditions: 50 mM MES, pH 6.7, 10 mM $MgCl_2$, and 2% glycerol, 37 °C. [c] $-RT \ln[K^{c^0}/K^{c^0}(\text{modified})]$ or $-RT \ln[k^{c^0}(\text{modified})/k^{c^0}]$. Negative: modified substrate/ribozyme is more efficient. Positive: modified substrate/ribozyme is less efficient. [d] Substrates with an A/U-rich 5′ leader sequence.

groove utilized in the P RNA reaction. This finding is consistent with the broader substrate selectivity of the holoenzyme: a smaller contact surface should allow the holoenzyme to recognize structures that are less similar to tRNA with comparable efficiency. The cleavage rate constant of a single modification is decreased by less than 3-fold (0.6 kcal/mol), suggesting that interactions with the T stem-loop mainly contribute to substrate binding.

Two substitutions of residues in P RNA known to contact tRNA directly are also tested with the holoenzyme (9230 and 9130 in Table 1). Both mutations affect the binding and cleavage to similar extents compared to the P RNA reaction. Therefore, at the minimum, there is significant overlap between the binding surface for tRNA in the ribozyme and the holoenzyme.

Substrate Modifications in the Region around the Cleavage Site. The important contributors in this region include the 5′ leader, the acceptor stem, and the 3′ CCA nucleotides of tRNA. 2′OH → 2′H modifications in the acceptor stem and in the 5′ leader have little effect on binding or cleavage (<0.6 kcal/mol; Table 2). Deletion of the 3′ CCA as well as mutation of the G1C72 base pair to other Watson−Crick base pairs substantially reduce binding and cleavage, consistent with previous proposals for the function of these residues (*1*, *22*−*25*). The small effect of 2′ deoxy substitutions in the acceptor stem is the same using substrates containing a 2′ ribo at the cleavage site (Table 3). Only the substitution of the 2′OH → 2′H at the cleavage site decreases binding and catalysis by a large margin of 0.9 and 2.0 kcal/mol, respectively. Unlike recognition of the T stem-loop, the results for the holoenzyme reaction are qualitatively identical to the P RNA reaction (*17*).

Effects of Holoenzyme on Miscleavage. The $tRNA^{Phe}$ substrate used in this work significantly miscleaves at nucleotides −2/−1 and +2/+3 (denoted as m^{-1} and m^2-cleavage sites, the correct cleavage site is referred to as c^0-site; ref *17*). This high extent of miscleavage has been attributed to the particular sequence of the yeast $tRNA^{Phe}$ used in our work (*17*). The miscleavage reaction (e.g., cleavage at the c^0-site versus the m^2-site) can be described as parallel binding events leading to distinct ES complexes along the reaction pathway:

Table 2: Effects of Substrate Modifications in the Region around the Cleavage Site

substrate[a]	K^{c^0} (μM)[b]	$\Delta\Delta G$ (kcal/mol)	k^{c^0} (min^{-1})[b]	$\Delta\Delta G$ (kcal/mol)
(d-1)	0.13 ± 0.03		0.42 ± 0.03	
d71	0.15 ± 0.04	0.0	0.44 ± 0.03	0.0
d72	0.14 ± 0.04	0.0	0.43 ± 0.03	0.0
d+1	0.09 ± 0.03	−0.2	0.18 ± 0.02	0.5
d+2	0.20 ± 0.03	0.3	0.40 ± 0.02	0.0
d+3	0.07 ± 0.01	−0.4	0.41 ± 0.02	0.0
d-3	0.05 ± 0.01	−0.6	0.56 ± 0.04	−0.2
d-2	0.22 ± 0.03	0.3	0.26 ± 0.01	0.3
ΔCCA	2.1 ± 0.1	1.7	0.080 ± 0.001	1.0
a1u72	1.1 ± 0.3	1.3	0.005 ± 0.001	2.7
c1g72	0.83 ± 0.06	1.1	0.12 ± 0.01	0.8
u1a72	2.6 ± 0.6	1.8	0.041 ± 0.003	1.4

[a] All substrates contain a 2′deoxy nucleotide (d-1) at the cleavage site. [b] Conditions: 50 mM MES, pH 6.7, 10 mM $MgCl_2$, and 2% glycerol, 37 °C.

Table 3: Effects of Substrate Modifications with Substrates Containing a 2′ Ribo Nucleotide at the Cleavage Site

substrate	K^{c^0} (μM)[a]	$\Delta\Delta G$ (kcal/mol)	k^{c^0} (min^{-1})[a]	$\Delta\Delta G$ (kcal/mol)
(r-1)	0.15 ± 0.05	*b*	2.6 ± 0.3	*b*
d+1	0.25 ± 0.06	0.3	1.6 ± 0.2	0.3
d+2	0.08 ± 0.02	−0.4	3.0 ± 0.2	−0.1
d+3	0.10 ± 0.01	−0.2	3.5 ± 0.2	−0.2
d-3	0.029 ± 0.004	−1.0	2.2 ± 0.1	0.1
5′aauau	0.06 ± 0.03	−0.6[c]	6.2 ± 0.4	−0.5[c]

[a] Conditions: 50 mM MES, pH 6.1, 10 mM $MgCl_2$, and 2% glycerol, 37 °C. [b] K^{c^0} and k^{c^0} for the C/G-rich 5′ leader substrate containing a 2′H at the c^0-site is 0.60 ± 0.10 μM and 0.081 ± 0.006 min^{-1} at pH 6.1, respectively. The 2′ ribo substrate is 0.9 and 2.0 kcal/mol more efficient in K^{c^0} and k^{c^0} than the 2′H substrate. [c] K^{c^0} and k^{c^0} for the A/U-rich 5′ leader substrate containing a 2′H at the c^0-site is 0.03 ± 0.01 μM and 0.41 ± 0.03 min^{-1} at pH 6.1, respectively. The 2′ ribo substrate is 0.4 kcal/mol less efficient in K^{c^0}, but 1.8 kcal/mol more efficient in k^{c^0} than the 2′H substrate.

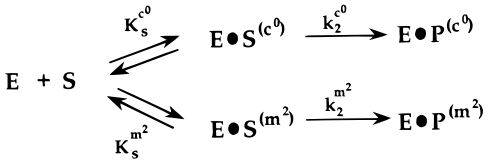

where $K^{c^0} = K^{m^2} = K_s^{c^0}/(1 + K_s^{c^0}/K_s^{m^2})$ and $k^{c^0} = k_2^{c^0}/(1 + K_s^{c^0}/K_s^{m^2})$; $k^{m^2} = k_2{}^{m^2}/(1 + K_s^{m^2}/K_s^{c^0})$ for the substrates containing a 2′ deoxy at the c^0-site ($K_s = k_{-1}/k_1$ and $k_2 \ll k_{-1}$; ref *26*). With a 2′ H at the c^0-site, k^{c^0} is favored over k^{m^2} and $k^{m^{-1}}$ by 20 and 14-fold (1.8 and 1.6 kcal/mol) at pH 6.7, respectively. With a 2′OH at the c^0-site, k^{c^0} is favored over k^{m2} and $k^{m^{-1}}$ by 10 and 3.4-fold (1.4 and 0.8 kcal/mol) at pH 6.1, respectively.

The effects of substrate modification on cleavage at different sites can be analyzed by comparing the cleavage rate constants, for example $k^{m2/m^{-1}}$ (unmodified)/$k^{m2/m^{-1}}$ (modified substrate) (Figure 4). Except for 53 and 54, modifications in the T stem-loop region have generally no effect on m^2-cleavage. 2′OH → 2′H substitutions at 53 and 54 improves m^2-cleavage by 0.8 kcal/mol over the unmodi-

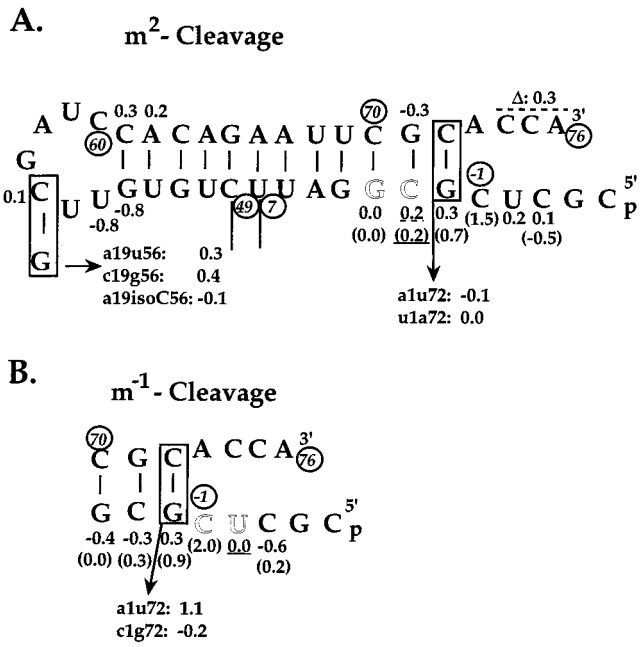

FIGURE 4: ΔΔG (+RT ln[$k^{m^2/m^{-1}}$(unmodified)/$k^{m^2/m^{-1}}$(modified)]) of 2′OH → 2′H modifications, 3′ CCA deletions and 1−72 and 19−56 base pair mutations on m^2 (A) and m^{-1} (B)-cleavage at 37 °C. Positive ΔΔ*G* values indicate that the modification decreases the cleavage rate constants; negative ΔΔ*G* vales indicate that the modification increases the cleavage rate constants. Only the top half and the 5′ leader of the pre-tRNA^{Phe} substrate are shown and the residue numbers are italicized and circled. The numbers below each residue are ΔΔ*G* values for substrates containing a 2′H at the c^0-site at pH 6.7. The numbers in the parenthesis are ΔΔG values for substrates containing a 2′OH at the c^0-site at pH 6.1. All reactions contain 10 mM $MgCl_2$ and 2% glycerol. The 2′OH → 2′H modifications at the m^2 and m^{-1} sites are underlined for their respective cleavage site. The cleavage sites are between the outlined nucleotides. The m^2-cleavage is more extensively analyzed due to better gel resolution.

fied substrate. Comparing the same modifications for c^0-cleavage (Table 1), each 2′OH group at 53 and 54 improves the fidelity for cleavage at the c^0-site by 1.0−1.2 kcal/mol. This result shows that high-affinity binding of the T stem-loop region can contribute to cleavage site selection in the holoenzyme.

In the region around the cleavage site, substitution of the 2′OH → 2′H at the c^0-site reduces cleavage at all sites to a similar extent (1.5−2.0 kcal/mol), whereas the 2′OH → 2′H modifications at the m^2- or m^{-1}-sites have only small effects (<0.3 kcal/mol) on cleavage at all sites (Figure 4). These results are very similar to the effects of modifications on the P RNA reaction (*17*). Changing the G1C72 pair to other Watson−Crick base pairs strongly reduces cleavage at the c^0-site (Table 2), but has little effect on m^2-cleavage, consistent with involvement of the G1C72 base pair specifically for the c^0-site. The base pair identity at 1−72 position also affects m^{-1}-cleavage, but to a lesser extent than c^0-cleavage. Deletion of the 3′ CCA has little effect on k^{m^2}, especially compared to the larger decrease observed in c^0-cleavage. Hence, the net effect of 3′ CCA deletion improves cleavage at m^2 compared to c^0 (Figure 4). These results are consistent with previous reports that mutations of the 3′ CCA influence the cleavage efficiency at different sites (*27*−*29*). An A/U-rich 5′ leader improves cleavage at c^0 compared to m^2 by less than 0.4 kcal/mol in the holoenzyme reaction (data not shown). These results are qualitatively similar to the effects of the same modifications on the P RNA reaction at high ionic strength (*17*), suggesting that the holoenzyme selects the cleavage site in a manner comparable to that of the P RNA reaction.

DISCUSSION

P Protein Binding to P RNA. The *B. subtilis* P protein induces protection of three regions of P RNA that are located in both folding domains. Regions 1 and 2 are in the domain responsible for binding of the T stem-loop of tRNA (*6*, *14*) and region 1 is located in a four-way junction present in all bacterial P RNAs (*30*). Region 2 contains both helical and nonhelical components and the nucleotides in the nonhelical region are conserved. Region 3 is in the other domain that contains the entire active site of P RNA (*7*, *9*, *31*). Protection of P RNA induced by the P protein could either be due to direct contacts or a conformational change in the P RNA or both. The requirement of both P RNA domains for hydroxyl radical protection by the P protein indicates that the protein contacts both domains. The three potential binding regions may be proximal in space to constitute a single binding surface or may be spatially distant to form two binding surfaces, presumably one in each domain. Alternatively, one or more of these three regions may be protected by an RNA conformational change induced by the protein binding. The crystal structure of the *B. subtilis* P protein shows at least two potential RNA-binding sites (*32*). Photo-cross-linking studies have mapped one binding site to directly contact the 5′ leader of a pre-tRNA substrate (S. Niranjanakumari and C. Fierke, unpublished data). We suggest that the other RNA-binding site contacts part or all of the binding surface on the P RNA.

Substrate Selectivity by the Holoenzyme. The holoenzyme cleaves the precursors of tRNA, the *E. coli* 4.5S RNA (*1*, *12*), and the C4 repressor RNA of coliphage P1 and P7 (33) with similar efficiencies (k_{cat}/K_m), whereas P RNA, at elevated ionic conditions, catalyzes the cleavage of pre-tRNA substrates much more efficiently than the precursor 4.5S RNA (*12*). The recognition pattern of the pre-tRNA substrate by the holoenzyme determined in this work provides a molecular rationale for these observations (Figure 5). The secondary structures of these substrates are quite different. The tRNA is composed of two coaxially stacked helices with a total of 12 base pairs followed by its specific tertiary structure. The 4.5S RNA and the C4 repressor RNA contain a single helix of at least 14 base pairs (*12*, *33*).

A groove formed by the tertiary structure of tRNA is recognized by the P RNA and by the holoenzyme, as shown previously for P RNA (*14*) and now in this work. Structurally, this groove begins from the minor groove of a standard A-form helix (the T stem) and extends into the edge of the tRNA structure where the 4-NH_2 of C56 is located. The top part of this groove is similar to the minor groove of an A-form helix, whereas the bottom part of this groove is uniquely defined by the tertiary structure of tRNA. Because of binding to the entirety of this groove (light gray oval in Figure 5), the P RNA alone reaction is more specific for pre-tRNA substrates. Other less tRNA-like biological substrates are unlikely to contain binding surfaces corresponding to this whole groove. On the other hand, the holoenzyme recognizes only a part of this groove, in particular, the region

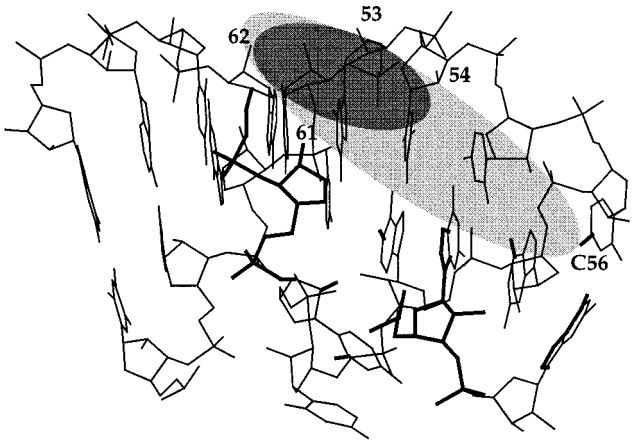

FIGURE 5: Rationalization for the broader substrate selectivity by the RNase P holoenzyme. The T stem-loop region of the $tRNA^{Phe}$ is shown with the frontal view of the groove containing the 2′OH groups of 53, 54, 61, 62, and the 4-NH_2 of C56. All five groups interact with P RNA as indicated by a light gray oval. The holoenzyme only interacts with the 2′OH groups of 53, 54, and 62 as indicated by a dark gray oval.

where it is more A-form like (dark gray oval in Figure 5). This modified recognition pattern allows the holoenzyme to recognize tRNA and other biological substrates in a similar fashion. However, a purely A-form helix may not work well for holoenzyme recognition, since the 2′OH of 54 is not part of a regular A-form helix. Both 4.5S RNA and the C4 repressor RNA have tandem U−G/G−U pairs at the equivalent position of the 53−61 base pair in tRNA. These U−G/G−U pairs may distort the A-form minor groove to mimic the top part of the groove in tRNA where holoenzyme recognition occurs.

Despite the potentially fewer contacts to the groove structure made by the holoenzyme, the overall affinity of holoenzyme binding to the tRNA component is still ∼9-fold better than binding by the P RNA under physiological conditions (*3*). This result may be explained by the potential shift of $K^{[Mg]}$ for the two Mg^{2+} ions involved in tRNA binding (*34*). Alternatively, P protein binding to both folding domains of P RNA fixes the orientation of these domains so that the binding surface in the holoenzyme can have a better fit to the tRNA structure. A third possibility involves direct contacts of the P protein to the tRNA component for this increased tRNA binding affinity.

Recognition of in Vitro Selected Substrates by the Holoenzyme. The broader substrate selectivity for the holoenzyme is manifest in a selection experiment (*13*) using either the *E. coli* M1 RNA alone or the *E. coli* holoenzyme. Substrates with more diverse secondary structures and hairpin loop sizes were obtained with the holoenzyme. Applying our binding model for the holoenzyme, the selected substrates should contain a common groove-like structure composed either of a distorted A-form helix or of a coaxially stacked acceptor stem/T stem-like helices with a terminal hairpin loop.

When the selection experiment was carried out with *B. subtilis* P RNA alone, four classes of substrates were isolated (*35*, *36*). Three of the four substrate classes have secondary structural motifs corresponding to the acceptor stem and the T stem-loop of tRNA with different loop sequences. Unlike tRNA, the linker regions connecting these helical motifs are not helical. Even though the selection was performed in the absence of the P protein, the holoenzyme can efficiently recognize all three substrates with only 2 or 5 nucleotides in the 5′ leader. Hence, the selected hairpin loop is likely to fold into a T stem-loop like structure for specific recognition. The fourth substrate class only contacts one of the two folding domains of P RNA at a site unrelated to tRNA binding (*7*). For this substrate with a three nucleotide 5′ leader, the T stem-loop binding site in P RNA is not needed and the holoenzyme and the P RNA bind with similar affinity, even under physiological conditions (A.L. and T.P., unpublished results).

Domain Orientation and Substrate Recognition. The observations that both the P protein and the substrate (*7*, *9*, *14*, *31*) likely contact both domains of P RNA suggest that the structural relationship of these domains may play a significant role in substrate binding. Both domains can fold independently and there is no evidence for strong interactions among these domains in the absence of substrate or P protein (*5*, *6*). Therefore, these domains may be inherently flexible relative to each other. Upon substrate binding, the domains likely become less flexible due to interactions with the substrate and the energetic penalty for reducing the mobility of the domains may decrease the apparent affinity of the ribozyme for the substrate. The binding of the P protein, however, may significantly reduce the flexibility of P RNA and lock the domains into an optimal orientation prior to binding of biological substrates. Such a domain-orientation effect may explain the similar affinity of both P RNA and holoenzyme for a selected substrate that interacts only with one domain (ref *7*; A.L. and T.P., unpublished results). The changes in domain flexibility and/or orientation cannot be discriminated from the hydroxyl radical protection pattern of the holoenzyme. We are now in the process of testing this hypothesis using biophysical techniques, e.g., small-angle X-ray scattering, that are sensitive to conformational changes on the scale of these domains.

Cleavage Site Selection by the Holoenzyme. The principle of cleavage site selection by the holoenzyme is identical to that of the P RNA reaction (*17*). The holoenzyme does not significantly change the extent of miscleavage at low ionic conditions (10 mM $MgCl_2$, pH 6.1−7.3) compared to P RNA cleavage at high ionic conditions (100 mM $MgCl_2$, 0.6 M KCl, pH 6.1−8.1). Like the P RNA reaction, the 2′OH → 2′H modification at the c^0-site has identically large effects on cleavage at all sites, whereas 2′OH → 2′H modifications at the m^2 and m^{-1} sites have no effect on cleavage at any site. This 2′OH(c^0) effect was attributed to its interaction with the ribozyme to increase the fraction of a hypothetical second ES complex on the reaction pathway (*17*). Two modifications affect cleavage at the m^2-site differently from cleavage at the c^0-site. The G1C72 mutations to other Watson−Crick base pairs have large effects on c^0-cleavage, while the same mutants display a much smaller effect on the m^2-cleavage (Figure 4). The nucleotide +1, therefore, can be considered as the equivalent of the −2 position for c^0-cleavage, where the base identity only plays a minor role. In the T stem-loop region, the 2′OH → 2′H modifications at 53 and 54 significantly improve m^2- over c^0-cleavage, suggesting that the interactions involving these 2′OH groups contribute less to the $ES^{(m^2)}$ complex. This result shows that the precise pattern of recognizing the T stem-loop region can influence cleavage at different sites.

Comparison of the RNase P Holoenzyme to Group I Intron Proteins. Several group I introns require specific proteins for splicing under physiological conditions. For the *Saccharomyces cerevisiae* CBP2 (*37*, *38*) and the *neurospora* CYT18 (*39*−*41*), hydroxyl radical protection of the intron core structure can only be detected with the bound protein. The functional role of these proteins is to stabilize the tertiary structure of the group I intron active site which is only folded at high [Mg^{2+}] or not at all in the absence of the protein. Hence, $K_{1/2}^{[Mg]}$ (folding) is equal to or higher than $K_{m}^{[Mg]}$ (splicing) for these group I introns. In contrast, the active site of P RNA is folded at much lower [Mg^{2+}] in the presence and absence of the P protein. Substrate binding and catalysis, on the other hand, require higher [Mg^{2+}], particularly for the P RNA reaction. Hence, $K_{1/2}^{[Mg]}$ (folding) is much lower than $K_{m}^{[Mg]}$ (catalysis) for P RNA. Several lines of evidence suggest that the folded P RNA structure detected by the hydroxyl radical protection is a "true" catalytic form. (i) An in vitro selected substrate is efficiently cleaved under physiological conditions with the P RNA or the holoenzyme (ref *7*; A.L. and T.P., unpublished results). (ii) The folded P RNA at 2−10 mM $MgCl_2$ is instantaneously active upon mixing with the pre-tRNA substrate (*16*), suggesting that there is no slow folding barriers after the Fe(II)-EDTA detected tertiary structure is formed. (iii) No discernible differences can be observed in hydroxyl radical protection at 5 mM and 100 mM Mg^{2+} (A.L. and T.P., unpublished results). These data, combined with functional analysis of the P protein (*3*, *4*, *15*), indicate that the P protein may be evolved to specifically enhance binding and catalysis of biological substrates.

ACKNOWLEDGMENT

We thank Professor Scott Strobel for the isoC phosphoramidite. We also thank Jeff Kurz, Sharon Crary and one reviewer for thoughtful comments on this manuscript.

REFERENCES

1. Altman, S., Kirsebom, L., and Talbot, S. (1993) *FASEB J. 7*, 7−14.
2. Pace, N. R., and Brown, J. W. (1995) *J. Bacteriol. 177*, 1919−1928.
3. Kurz, J. C., Niranjanakumari, S., and Fierke, C. A. (1998) *Biochemistry 37*, 2393−2400.
4. Crary, S. M., Niranjanakumari, S., and Fierke, C. A. (1998) *Biochemistry 37*, 9409−9416.
5. Pan, T. (1995) *Biochemistry 34*, 902−909.
6. Loria, A., and Pan, T. (1996) *RNA 2*, 551−563.
7. Pan, T., and Jakacka, M. (1996) *EMBO J. 15*, 2249−2255.
8. Talbot, S. J., and Altman, S. (1994) *Biochemistry 33*, 1399−1405.
9. Westhof, E. Wesolowski, D., and Altman, S. (1996) *J. Mol. Biol. 258*, 600−613.
10. Gopalan, V. Baxevanis, A. D., Landsman, D., and Altman, S. (1997) *J. Mol. Biol. 267*, 818−829.
11. Reich, C., Olsen, G. J., Pace, B., and Pace, N. R. (1988) *Science 239*, 178−181.
12. Peck-Miller, K. A., and Altman, S. (1991) *J. Mol. Biol. 221*, 1−5.
13. Liu, F.-Y., and Altman, S. (1994) *Cell 77*, 1093−1100.
14. Loria, A., and Pan, T. (1997) *Biochemistry 36*, 6317−6325.
15. Niranjanakumari, S., Kurz, J. C., and Fierke, C. A. (1998) *Nucleic Acids Res. 26*, 3090−3096.
16. Pan, T., and Sosnick, T. R. (1997) *Nat. Str. Biol. 4*, 931−938.
17. Loria, A., and Pan, T. (1998) *Biochemistry 37*, 10126−10133.
18. Scaringe, S. (1996) Ph.D. Thesis, University of Colorado at Boulder, Boulder, CO.
19. Strobel, S. A., and Cech, T. R. (1996) *Biochemistry 35*, 1201−1211.
20. Gait, M. J., Pritchard, C., and Slim, G. (1991) in *Oligonucleotides and analogues: A practical approach* (Eckstein, F., Ed.) pp 25−48, Oxford University Press.
21. Beebe, J. A., and Fierke, C. A. (1994) *Biochemistry 33*, 10294−10304.
22. Svard, S. G., and Kirsebom, L. A. (1993) *Nucleic Acids Res. 21*, 427−434.
23. Kirsebom, L. A., and Svard, S. G. (1994) *EMBO J. 13*, 4870−4876.
24. LaGrandeur, T. E., Huttenhofer, A., Noller, H. F., and Pace, N. R. (1994) *EMBO J. 13*, 3945−3952.
25. Oh, B.-K., and Pace, N. R. (1994) *Nucleic Acids Res. 22*, 4087−4094.
26. Fersht, A. (1985) in *Enzyme structure and mechanism*, 2nd ed., pp 109−111 and 137−138, W. H. Freeman and Company, New York.
27. Svard, S. G., and Kirsebom, L. A. (1992) *J. Mol. Biol. 227*, 1019−1031.
28. Kufel, J., and Kirsebom, L. A. (1996) *J. Mol. Biol. 263*, 685−698.
29. Kufel, J., and Kirsebom, L. A. (1996) *Proc. Natl. Acad. Sci. U.S.A. 93*, 6085−6090.
30. Haas, E. S., Brown, J. W., Pitulle, C., and Pace, N. R. (1994) *Proc. Natl. Acad. Sci. U.S.A. 91*, 2527−2531.
31. Harris, M. E., Kazantsev, A. V., Chen, J.-L., and Pace, N. R. (1997) *RNA 3*, 561−576.
32. Stams, T., Niranjanakumari, S., Fierke, C. A., and Christianson, D. W. (1998) *Science 280*, 752−755.
33. Hartmann, R. K., Heinrich, J., Schlegl, J., and Schuster, H. (1995) *Proc. Natl. Acad. Sci. U.S.A. 92*, 5822−5826.
34. Beebe, J. A., Kurz, J. C., and Fierke, C. A. (1996) *Biochemistry 35*, 10493−10505.
35. Pan, T. (1995) *Biochemistry 34*, 8458−8464.
36. Odell, L. T., Huang, V., Jakacka, M., and Pan, T. (1998) *Nucleic Acids Res. 26*, 3717−3724.
37. Weeks, K. M., and Cech, T. R. (1995) *Biochemistry 34*, 7728−7738.
38. Weeks, K. M., and Cech, T. R. (1996) *Science 271*, 345−348.
39. Mohr, G., Caprara, M. G., Guo, Q., and Lambowitz, A. M. (1994) *Nature 370*, 147−150.
40. Myers, C. A., Wallweber, G. J., Rennard, R., Kemel, Y., Caprara, M. G., Mohr, G., and Lambowitz, A. M. (1996) *J. Mol. Biol. 262*, 87−104.
41. Caprara, M. G., Mohr, G., and Lambowitz, A. M. (1996) *J. Mol. Biol. 257*, 512−531.

BI9816507